Stratigraphy, Geochemistry, and Paleomagnetism of Late Quaternary Bedrock and Paleosols, Karisoke Area, Virunga Mountains, Northwestern Rwanda

WILLIAM C. MAHANEY, RONALD G. V. HANCOCK & RENÉ W. BARENDREGT *)

Quaternary, stratigraphy, geochemistry, palaeomagnetic research,
Africa, Northwestern Rwanda, Virunga Mountains

Abstract: A surface soil and two buried paleosols, units II-III-IV (upper) and IV (lower)-V, provide important information on paleoclimate/drainage in the Virunga Mountains from drier to wetter paleoclimatic episodes of the last glaciation and middle postglacial periods. In general, the stratigraphy indicates a period of bedrock weathering, followed by episodic emplacement of tuffaceous sediments accompanied by weathering initially in a drier and perhaps colder paleoenvironment. Later, during the last glaciation (interstadial), increased stream activity emplaced alluvium, covered with a thin layer of tuff, all of which is weathered more vigorously than the underlying sediments. The surface soil (ground soil) shows comparatively less weathering and movement of mobile elements indicating the late middle to late Holocene paleoenvironment was somewhat drier and perhaps cooler compared with the early Holocene. The geochemistry of these three soils shows considerable depletion of Na, Ca, and K in the middle paleosol relative to the older buried paleosol and to the surface horizons. Iron is an important indicator of paleoclimate, suggesting that the middle II and III units of the upper paleosol formed under a paleoclimate wetter than today. The radiocarbon-dated middle paleosol indicates it could have been exposed to subaerial weathering from the Kalambo Interstadial (≈ 25,000 yr BP) to the middle Holocene. The total weathering in the middle unit is too advanced to have occurred during the Holocene. The relatively high concentrations of Th in local bedrock, tuffs, alluvium and slope wash indicate that it is the source of radioactivity reported by other workers in The Virunga Mountains.

[Stratigraphie, Geochemie und Paläomagnetik spätquartärer Gesteine und Paläoböden im Karisoke-Gebiet der Virunga-Berge, Nordwest-Rwanda]

Kurzfassung: Ein rezenter Boden und zwei begrabene Paläoböden, Einheiten II-III-IV (oberer) und IV (unterer)-V, liefern wichtige Informationen über Paläoklima und Abflußverhältnisse in den Virunga-Bergen von trockeneren zu feuchteren paläoklimatischen Phasen des Spätglazials bis zu mittleren postglazialen Zeiten. Zusammenfassend betrachtet, weist die stratigraphische Abfolge zunächst auf eine Verwitterungsperiode des Festgesteins hin, der eine Phase folgt, in der tuffige Schichten abgelagert wurden. Die Zeit war von einer Verwitterung unter trockeneren und vielleicht kälteren Bedingungen begleitet. Später, während des letzten Glazials, kam es bei verstärkter Aktivität der Flüsse zur Sedimentation von Schwemmlandablagerungen, die von einer dünnen Tuff-Schicht überdeckt wurden. Diese Sedimente sind intensiver verwittert als die liegenden Schichten. Der rezente Boden zeigt eine vergleichsweise geringe Verwitterung mobiler Elemente, was darauf hindeutet, daß die Klimaverhältnisse im späten Mittel-Holozän und Spät-Holozän etwas trockener und vielleicht kühler waren als im Früh-Holozän. Die Geochemie der drei Böden zeigt eine bedeutende Abnahme von Na, Ca und K im mittleren Paläoboden im Vergleich zum älteren Paläoboden und zu den rezenten Böden. Eisen als ein wichtiger Indikator für das Paläoklima deutet darauf hin, daß die mittleren Einheiten II und III des oberen Paläobodens unter feuchteren Klimabedingungen als heute entstanden sind. Die Radiokarbon-Datierungen des mittleren Paläobodens zeigen, daß dieser Boden einer subaerischen Verwitterung vom Kalambo-Interstadial (≈ 25 000 Jahre vor heute) bis zum Mittel-Holozän ausgesetzt war. Die gesamte Verwitterung im mittleren Abschnitt ist zu weit fortgeschritten und während des Holozäns entstanden. Die relativ hohe Konzentration von Th in den anstehenden Festgesteinen, Tuffen, Schwemmlandsedimenten und Hangrutschmassen zeigt, daß Th die Quelle der Radioaktivität ist, von der andere Autoren aus den Virunga-Bergen berichten.

*) Adresses of the authors: Prof. Dr. WILLIAM C. MAHANEY, Geomorphology and Pedology Laboratory, Department of Geography, Atkinson College, York University North York, Ontario, Canada M 3 J 1 P 3. Dr. R. G. V. HANCOCK, SLOWPOKE Reactor Facility and Department of Chemical Engineering and Applied Chemistry, University of Toronto, Toronto, Ontario, Canada M 5 S 1 A 4. Prof. RENÉ W. BARENDREGT, Department of Geography, Lethbridge University, Lethbridge, Alberta, Canada T 1 K 3 M 4.

1 Introduction

The surficial geology and geochemistry of the Virunga Mountains in northwestern Rwanda are very poorly understood (ANTRUN and MAGNEE 1983; HARRIS 1982). Of the five Rwandan volcanoes, Karisimbi (4510 m) is the highest and contains a complex series of lava flows which cover the largest area. Over 150 parasitic cones circle the summit area and presumably are the source of most pyroclastic sediments and rocks found around the mountain. One young lava flow (precise location unrecorded) from Karisimbi has been dated 56,000 yr by K/Ar (HARRIS 1982). The following discussion concerns the stratigraphy, geochemistry and paleomagnetism of a section on the northeastern flank of Karisimbi (Figure 1) at 3100 m (in the valley area between Karisimbi and Visoke).

2 Field Area

The Virunga Volcanoes in northwestern Rwanda (on the Zaire-Rwanda-Uganda border Figure 1), consist mainly of rocks of basaltic composition (MERCIER 1984). In some cases, thick cover over rocks of tuffaceous origin overlie the basalt; all are usually weathered to depths of 1.0 to 3.0 m depending on age. Surficial deposits of loess, colluvium and alluvium are often weathered into thick (≈ 2.0 m) brown (10 YR 4/4) colored paleosols sometimes forming compound units (e.g. similar to IIA11b and IIA12b horizons in Figure 2) that appear to have formed during the last glaciation when the timberline was depressed several hundred meters.

The site is located in the upper portion of the Hagenia woodland dominated by *Hagenia abyssinica* (COE 1967; HEDBERG 1964). The presence of a dark moorland-like paleosol, at or near the surface, that can be traced to elevations as low as 2750 m indicates a substantial vegetation depression. Because the thick moorland-like paleosol is similar to one observed on Mount Kenya (900 km to the east) (MAHANEY 1990), it is considered an important paleoclimatic indicator. The present-day climate is wet with mean annual precipitation at approximately 2000 mm (FOSSEY 1982). Evapotranspiration is unknown. The temperature in the upper Hagenia forest may approximate the mean annual temperature of $10 \pm 6\,°C$ at a similar altitude on Mount Kenya (MAHANEY & BOYER 1986).
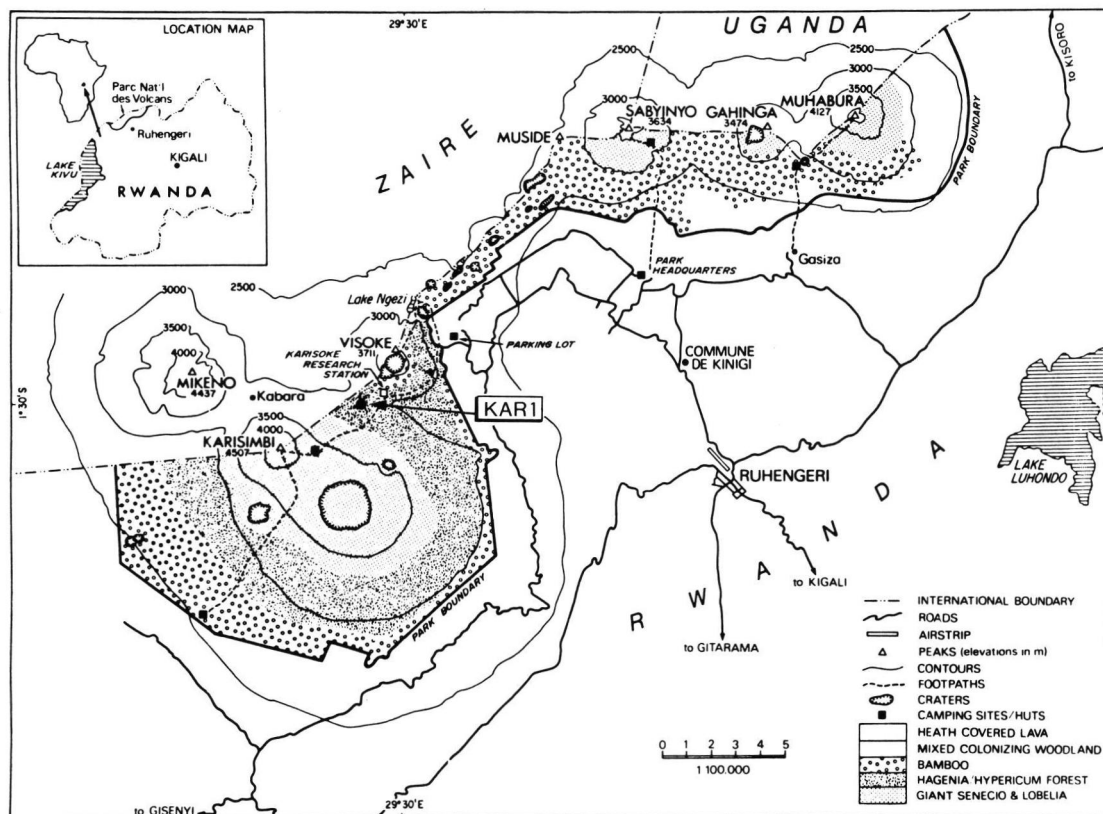

Fig. 1: Location of sampling site in the Virunga Mountains, northwestern Rwanda.

3 Methods

The KAR 1 section was described using the nomen-clature of the SOIL SURVEY STAFF (1951, 1975) and BIRKELAND (1984). Soil and sediment colors were estimated using the color chips of OYAMA & TAKE-HARA (1970). Samples were collected and dried after removing the granule and pebble size material (> 2 mm). Particle size determinations follow the Wentworth scale (FOLK 1968) for coarse material (sand and silt) and the SOIL SURVEY STAFF (1975) for fine particles (clay). Particle sizes were determined by dry sieving for coarse material (2 mm—63 μm) (DAY 1965) and by sedimentation for fines (< 63 μm) (BOUYOU-COS 1962). Each sample was X-rayed using Ni-filtered Cu Kα radiation to determine the mineral content of the < 2 μm fraction following procedures outlined by WHITTIG (1965) and MAHANEY (1981). Salts were analyzed following procedures of BOWER & WILCOX (1965). The pH was measured by electrode using a soil-water ratio of 1 : 5. The < 2 mm samples were subsampled and approximately 1 to 2 g was placed in small flip-top polyvials for neutron activation analysis in the SLOWPOKE nuclear reactor at the University of Toronto (HANCOCK 1978, 1984).

To determine the concentrations of U, Dy, Ba, Ti, Mg, Na, V, Al, Mn, Ca and K, which produce short-lived radioisotopes, the samples were irradiated se-rially for 1 minute at a neutron flux of 1.0×10^{11} n·cm^{-2}·s^{-1} in the SLOWPOKE nuclear reactor at the University of Toronto. After a delay time of 19 minutes (which allows the very short-lived ^{28}Al to decay to acceptable levels), each sample was assayed using 5 minute counts with on-site gamma-ray spec-trometers, as described by HANCOCK (1984). Appro-priate gamma-ray peak areas were measured and the chemical concentrations calculated using the compara-tor method.

The samples were then batch irradiated for 16 hours at a neutron flux of 2.5×10 n·cm^{-2}·s^{-1}, and after a waiting time of approximately 7 days the concentra-tions of Sm, U, Yb, La, As, Sb, Br, Sc, Fe and Na were similarly determined, with the Na giving a cross-check with the first analysis. After a two-week delay, the samples were recounted and the concentrations of Nd, Ce, Lu, Ba, Th, Cr, Hf, Sr, Cs, Ni, Th, Sc, Rb, Fe, Co, Ta and Eu were measured. Once again, the Sc and Fe were used to cross-check the second phase of the analysis.

4 Results and Discussion

4.1 Stratigraphy

A sequence of slope wash and alluvium, interbedded tuffs, and basalt that is presumably younger than

$\approx$ 50,000 yr (HARRIS 1982) provided an opportunity to study weathering and paleosol genesis in a humid tropical setting over a short span of time. The weath-ered basalt and tuff (units V and IV) shown in Figure 2 are exposed in a gully along the lower flanks of Kari-simbi Volcano. Because the two lower units were less highly weathered (based mainly on color differences observed in the field), it was inferred that they had formed over a short span of time followed by a longer period of weathering which produced hues as brown as 10 YR 6/3. Unit III appeared to be more highly altered with colors of 10 YR 4/6 indicating that Fe-hydroxides and oxides might make up the bulk of the weathering products. Because the lower two stratigra-phic units consist of pyroclastic/volcanic rock materials that were at least altered to a moderate degree on a flow surface dated at $\approx$ 50,000 yr, it is believed they might have weathered during the drier paleoclimate which accompanied the early stadial of the last glacia-tion $\approx$ 50,000—35,000 yr BP) (MAHANEY, 1990).
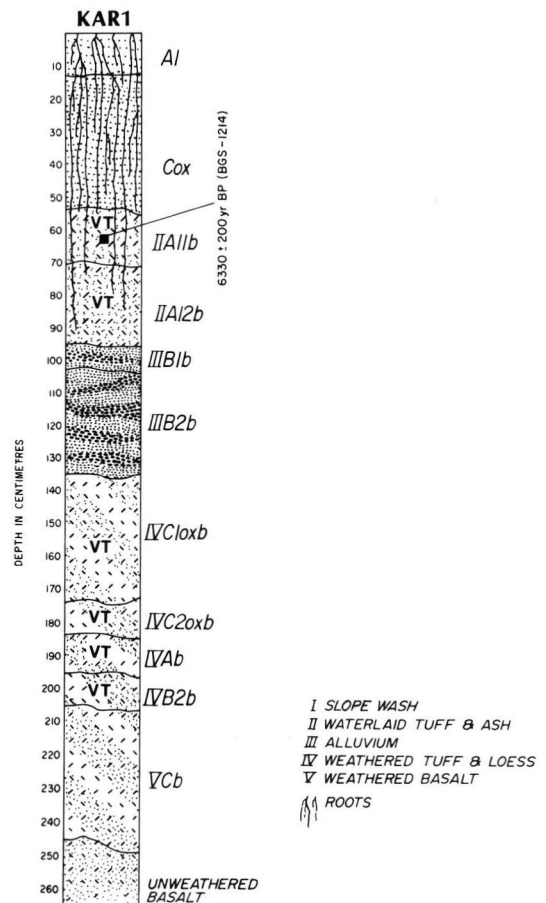

Fig. 2: Stratigraphy of the KAR 1 section,
Virunga Mountains.

The overlying units (I, II and III), consisting of slope wash, alluvium and waterlaid tuff, are considerably younger judging by a ^{14}C date of 6330 ± 200 yr BP (BGS — 1214) on charcoal in the IIA11b horizon. Because the precipitation is so high, the particle size so coarse (Table 1), and roots prevalent in the upper two units (Figure 2), it is highly likely that some downward movement of geobiochemical contaminants might have occurred. Units II and III appear to have formed through the interstadial of the last glaciation (Kalambo), the last glacial maximum and early to middle Holocene.

The particle size data in Table 1 show some important trends with respect to clay and silt that bear on the morphogenesis of the two buried paleosols. The lower paleosol [units IV (lower) and V] is considerably higher in silt compared with the weathered bedrock which might be related either to the airfall influx of tuffs and/or loess (glacially-crushed quartz grains indicate aeolian transport of sediments from the Ruwenzori Mountains or some other glaciated area; MAHANEY 1990) from the nearby Ruwenzori Mountains or to reworking of locally derived silt following a major vegetation belt depression during colder stadial climate at or near the end of the last glaciation. Clay translocation in this lower paleosol is only on the order of 1 % indicating a drier paleoclimate that was not conducive to the downward movement of fine-grained particles.

The upper paleosol units [(II, III, and IV (upper)] also contain high silt relative to the surface slope wash unit and the weathered bedrock (V). As in the lower paleosol this increase could be related to the emplacement of pyroclastic material or to sorting and reworking of older sediments by streams. The increase of percent clay in the IIA11b and IIIB2b horizons indicates a paleosol with considerable power to form clay relative to the underlying paleosol. This increase of clay in the IIIB2b horizon supports the hypothesis of increased downward movement relative to the lower and upper units in the sequence. Because the surface soil is formed in slope wash reworked from nearby slopes covered with pyroclastic sediments it is possible only to point out that higher sand percentages suggest sufficiently high surface run off to move coarse-grained sediments; increasing silt and clay with depth indicate the possibility of some downward movement.

4.2 Mineralogy

In order to test the hypothesis of a young ($< 50,000$ yr) age for the paleosols in the KAR1 sequence we analyzed the mineralogy of the $< 2 \mu m$ fraction in each horizon. In the oldest buried paleosol only a trace amount of illite was detected in the IVB2b. Quartz is present in all horizons with moderate amounts in the VCb and IVB2b horizons diminishing somewhat in the IVAb horizon. Volcanic feldspars (mainly anorthoclase) are present in small amounts throughout with somewhat lower reflections in the IVAb horizon. Small amounts of hematite were also detected.

The mineralogy of the upper paleosol shows a similar absence of clay minerals with hematite appearing in small to trace quantities as the chief weathering product. Quartz is highest in unit II and in the IVC2oxb (moderate amounts) horizons. Volcanics feldspars are highest in the IIA11b, IIA12b, and IIIB1b horizons, declining somewhat in the lower horizons. The ground soil is noticeably different in that quartz (abundant amounts) and volcanic feldspars (small amounts) are higher than in the two buried paleosols.

Table 1: Particle size ratios for horizons in the KAR1 paleosol sequence, Virunga Mountains, Northwestern Rwanda

Horizon	Depth (cm)	Sand (%) (2 mm—63 μm)	Silt (%) (63—2 μm)	Clay (%) (< 2 μm)
A1	0— 13	82.4	11.1	6.5
Cox	13— 54	66.8	25.5	7.7
IIA11b	54— 70	43.0	42.3	14.7
IIA12b	70— 94	56.4	36.8	6.8
IIIB1b	94—103	75.0	22.4	2.6
IIIB2b	103—135	29.3	59.4	11.3
IVC1oxb	135—173	35.7	57.8	6.5
IVC2oxb	173—182	82.1	15.7	2.2
IVAb	182—195	45.7	48.9	5.4
IVB2b	195—205	42.1	51.6	6.3
VCb	205—245	65.4	32.2	2.4

Table 2: Dry colors, pH and total salts in paleosol sequence KAR 1, Virunga Mountains, Northwestern Rwanda

Horizon	Depth (cm)	Dry[a] Color	pH (1 : 5)	E. C.
A 1	0— 13	10 YR 2/2 2/3	5.0	.28
Cox	13— 54	10 YR 4/3 4/2	5.5	.05
II A 11 b	54— 70	10 YR 3/3	5.3	.09
II A 12 b	70— 94	10 YR 3/4	5.4	.05
III B 1 b	94—103	10 YR 5/3	5.4	.05
III B 2 b	103—135	10 YR 4/6	5.5	.04
IV C 1 oxb	135—173	10 YR 7/3	5.5	.06
IV C 2 oxb	173—182	10 YR 6/3	5.8	.04
IV A b	182—195	10 YR 3/4	5.8	.08
IV B 2 b	195—205	10 YR 6/3	5.8	.04
V C b	205—245	10 YR 6/3 5/3	5.8	.07

[a] Colors follow Oyama and Takehara (1970)

Also, pyroxene which exists in trace amounts in the buried paleosols is higher in the ground soil. Because quartz is relatively rare in the volcanic rocks of the Virunga Mountains it may signal airfall influx, perhaps, from the nearby Ruwenzori Mountains. The plagioclase feldspars are noticeably higher in the A 1 horizon when compared with the lower paleosols and with the Cox horizon indicting they are being contributed from fresh outcrops up slope. Although it may be inappropriate to compare the $< 2\,\mu m$ fraction mineralogy with the $< 2\,mm$ fraction geochemistry, elevated Na and K concentrations are also observed in the A 1 and Cox horizons (see Table 3).

4.3 Soil Chemistry

Soil colors, pH and total salts (Table 2) were studied to determine whether they could be used to differentiate the three units. The pH trends in the upper two units show slight increases with depth; the lower unit is uniform. These data indicate slight movement of H^+ ions in the upper two units and none in the lower unit. The data for total salts reveal only slightly higher concentrations in the A and Ab horizons relative to the other horizons. Based on the geochemical data discussed later the salts present must be NO and SO rather than Cl. The soil colors shown in Table 2 are all in the 10 YR range suggesting younger material that is not highly altered. These yellowish red colors are compatible with the liberation of moderate amounts of goethite and minimal to trace amounts of hematite. The color trends suggest that the III B 2 b horizon might contain the highest concentration of liberated

oxides, hydroxides and clay minerals. Table 3 confirms this prediction with its highly elevated Fe content in the III B 2 b horizon.

4.4 Geochemistry

The chemical analysis data for the KAR 1 section, which are listed in Table 3, show considerable variability. Some of the variation may be associated with different lithological materials or with weathering, paleoclimate and/or drainage. Because Na and K are the most mobile of the major elements their depletion in the tuff/ash, alluvium, and lower tuff/loess horizons indicates that weathering effects were especially prominent in forming these Inceptisols. This supposition is born out by a check of the inter-element correlations using Pearson correlation coefficients, which show that Na and K are highly positively correlated. Both are positively correlated with Rb and are negatively correlated with Sc, T, Cr, Ni, Br and Cs.

Four other correlation groups including major elements are also apparent. Magnesium, Ca, Mn, Co, V, Sr, Cl, and Ba are all highly positively correlated and are negatively correlated with As, Sb, Br, the rare earth elements (REEs), Hf, Ta, Th, and U. Aluminium is positively correlated with As, Sb, the REEs, Hf, Ta, Th, and U, and is negatively correlated with Cr, Sc, V, Ti, Mn, and Co. Titanium, Sc, V, Cr, Ni, and Mn are all highly positively correlated and are negatively correlated with As, Sb, REEs, Hf, Th, and U. Iron does not correlate with any of the other major elements, although it is negatively correlated with Sb, the REEs, Hf, Ta, Th, and U.

Table 3: Geochemistry of the < 2 mm fraction of Section KAR 1, Karisoke Area, Virunga Mountains, Northwestern Rwanda

Lithology	Horizon	Depth (cm)	Na (%)	Mg (%)	Al (%)	Cl (ppm)	K (%)	Ca (%)	Sc (ppm)	Ti (ppm)	V (ppm)	Cr (ppm)	Mn (ppm)	Fe (%)	Co (ppm)	Ni (ppm)	As (ppm)	Br (ppm)	Rb (ppm)	Sr (ppm)	Sb (ppm)	Cs (ppm)	Ba (ppm)	La (ppm)	Ce (ppm)	Nd (ppm)	Sm (ppm)	Eu (ppm)	Tb (ppm)	Dy (ppm)	Yb (ppm)	Lu (ppm)	Hf (ppm)	Ta (ppm)	Th (ppm)	U (ppm)
Slope wash	A1	0— 13	2.00	2.0	7.8	440	4.1	5.0	15.4	18200	270	122	1480	8.14	33.0	<28	<1.9	6.0	122	1040	<.17	1.1	1260	98	171	50	9.6	2.73	1.1	3.4	2.2	0.30	7.14	9.1	21.4	3.8
	Cox	13— 54	2.19	1.3	8.7	510	3.2	3.8	13.2	13000	187	84	1210	6.63	25.7	<27	2.6	11.0	114	910	.19	1.0	1160	126	218	62	11.8	2.89	1.1	4.0	2.5	0.36	8.64	10.1	30.8	5.4
Tuff & ash	IIA11b	54— 70	1.07	1.1	6.6	240	1.7	2.9	14.6	15200	208	167	1020	6.21	26.2	<32	<2.1	10.9	81	490	<.18	2.4	870	99	189	51	8.9	2.41	1.1	3.7	2.0	0.33	7.58	11.4	24.8	4.9
	IIA12b	70— 94	0.80	1.0	7.7	<200	1.5	2.3	14.9	17800	250	154	765	4.77	15.1	<29	3.3	16.3	62	300	<.17	1.9	730	101	173	68	10.8	2.86	1.1	4.3	1.7	0.24	7.90	15.6	30.1	7.1
Alluvium	IIIB1b	94—103	0.82	1.1	8.8	<200	1.5	2.6	19.6	19300	299	195	605	4.76	13.6	38	3.1	15.1	53	340	<.18	1.0	670	123	227	54	13.4	3.75	1.4	5.5	1.8	0.28	9.75	16.0	32.8	7.6
	IIIB2b	103—135	1.42	0.5	8.4	<250	2.7	1.6	9.5	9000	178	47	639	14.9	15.7	<31	4.3	10.2	103	420	<.17	0.7	810	113	199	57	9.7	2.93	1.1	4.2	1.8	0.31	8.99	11.7	35.8	6.7
Tuff & loess	IVC1oxb	135—173	3.09	0.6	10.4	<200	4.5	1.2	6.5	5700	79	29	254	2.77	5.4	<25	5.2	9.1	179	270	.36	1.2	460	90	180	56	10.1	2.51	1.1	4.7	1.7	0.37	15.3	15.6	63.9	10.9
	IVC2oxb	173—182	1.77	0.9	9.6	530	3.5	3.3	10.2	12900	195	53	1130	7.88	22.4	<24	2.1	3.2	96	850	<.15	0.4	1170	111	197	57	10.0	2.75	1.0	3.9	2.1	0.32	8.98	9.7	31.3	4.8
	IVAb	182—195	1.18	0.4	10.3	<200	2.1	1.0	8.9	7700	125	45	354	3.98	16.1	<27	3.6	17.4	73	340	.34	0.5	640	215	330	87	15.8	2.81	1.5	7.3	3.0	0.48	13.3	12.2	59.9	14.5
	IVB2b	195—205	0.85	0.57	9.7	<200	2.1	0.8	11.5	16400	139	89	230	2.36	8.7	<29	3.4	9.5	154	150	.30	3.8	750	178	370	95	14.9	2.43	1.8	7.4	3.0	0.47	12.8	22.0	56.9	13.4
Basalt	VCb	206—245	2.20	0.9	10.9	<350	3.2	3.1	11.4	12600	178	45	733	4.88	16.3	<25	2.2	6.9	95	770	<.16	0.4	1260	94	182	59	10.5	2.90	1.2	3.8	2.3	0.32	11.2	11.9	41.0	6.4

If it is possible to relate these geochemical correlation findings to the specific mineralogy of the section, then there are significant quantities of at least five primary minerals combined to make up the sediments in the KAR 1 section.

The Na and K are depleted in the tuff and ash, in the alluvium, in the lower two horizons (IVAb and IVB2b) in the tuff and loess, indicating major leaching of these materials during or after their formation. The Mg, Ca, et al.-rich materials are highest in the slope wash material, in the IVC2oxb horizon in the tuff and loess, and in the weathered basalt horizon (VCb). Aluminium and its associated elements tend to increase in concentration downward through the section, with exceptionally high levels in the IVC1oxb horizon in the tuff and loess. Titanium and the associated transition metals tend to be depleted in the IIIB2b horizon in the alluvium and in the next lower IVC1oxb horizon in the tuff and loess, and in the IVAb horizon in the tuff and loess. They therefore tend to be depleted in the highest silt-containing units of the section, implying that they may be associated with material in either the sand or the clay fractions of the soils.

The distribution of Fe with depth shows trends that are probably related to paleoclimate and time of exposure to subaerial weathering processes. The highest Fe content, by far is found in the IIIB2b horizon in the alluvium. This high Fe content could result from differences in parent materials or from relative movement (depletion/enrichment) caused by different paleoclimates. The Fe levels are next highest in the slope wash material, and in the IVC2oxb horizon in the tuff and loess. If one compares the two buried paleosols [(II, III, and IV (upper)) and (IV (lower) and V)], it appears that the lower one was exposed for either a shorter time or that it formed in a paleoclimate with less available moisture than the upper one. It is likely that some of the Fe is organically complexed into a soluble form (see paleosol colors in Table 2), which allowed it to move downward in the upper buried paleosol, eventually enriching the buried B horizon. If this hypothesis is correct one is dealing with a considerably stronger paleoclimate in units II, III and IV (upper) compared with IV (lower) and V. The Fe data tend to support the notion that the lower paleosol formed during one of the stadial intervals during the last glaciation, while the upper paleosol formed mainly during the Kalambo Interstadial, Last Glacial Maximum, and early postglacial period up to around 6330 ± 200 yr BP (BGS-1214). While paleoecological data are scarce from the East African mountains, the period from 8000—4000 yr BP is considered to have been wetter and warmer than the early and later Holocene (MAHANEY 1988, 1989).
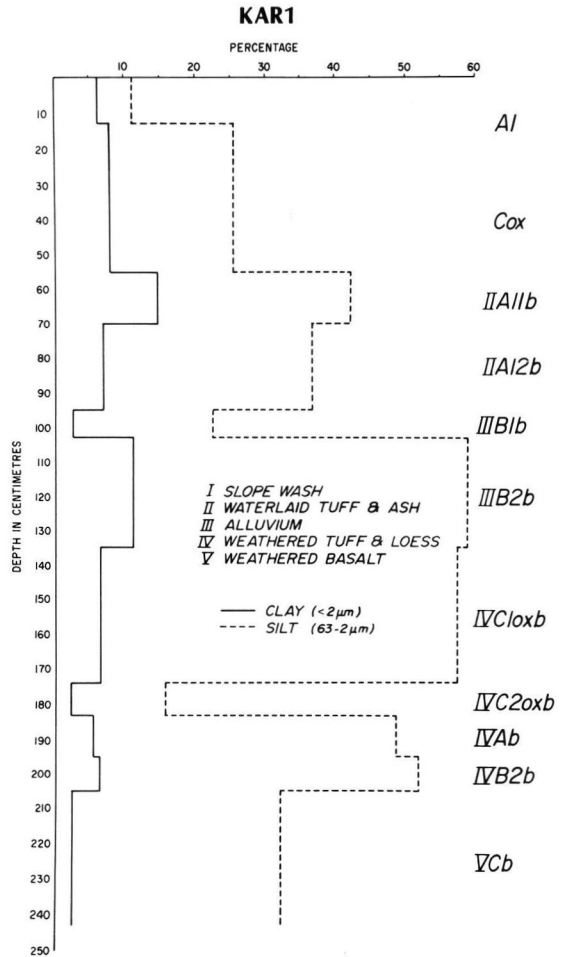

Fig. 3: Clay and silt distributions with depth in the KAR 1 section.

The high concentrations of U and Th through the surface soil and buried paleosols support the scanty information on radioactive basalts discovered during a geophysical survey in the Virunga Mountains during the early 1980's (ANTUN & MAGNEE 1983). Levels of U and Th are highest in the tuff and loess.

A chondrite normalized plot of the rare earth elements for the sample suite shows relative uniformity both in curve shape and in magnitude (see Figure 4). In this figure, the outermost data points are shown with solid black lines and the profiles for representative samples A1, Cox, and IVAb are included for detail.

The relative uniformity of the pattern indicates that the < 2 mm soil (paleosol) fraction samples were formed from material of similar magmatic composition, probably over a short geological time span.
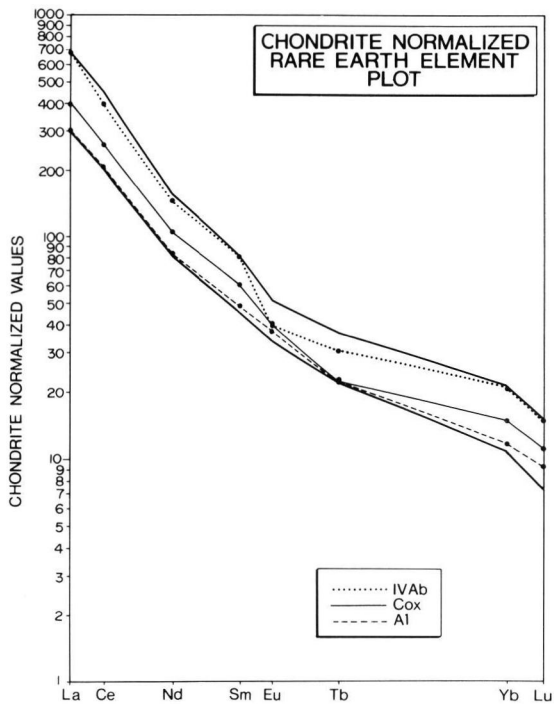
Fig. 4: Chondrite-normalized values for rare-earth elements
in selected paleosol samples from the KAR 1 section,
Virunga Mountains.

4.5 Paleomagnetism

In July, 1987, samples for paleomagnetic analysis were collected between Visoke and Karisimbi volcancoes (Figure 1). In total, 73 polycarbonate cubes (2 cm × 2 cm × 2 cm) were inserted into the sediments using hand pressure, and where necessary through gentle tapping with a rubber mallet. In addition, several blocks of unweathered vesicular basalt were marked and collected in the field, and cored in the laboratory using a bench drill. Analysis was carried out using a DSM-1 spinner magnetometer in the paleomagnetic laboratory at the Pacific Geoscience Center.

Magnetization data for the Karisoke sediments fall into three types: (a) single component magnetization (specimen b, Figure 5); (b) multicomponent magnetization (specimen c, Figure 5); and (c) incoherent magnetization (specimens a and d, Figure 5).

Approximately one third of the pilot specimens (Figure 5) collected from the Karisoke sediments can be characterized as a Type A magnetization, that is, they are single component (except for a small present earth's field component) and their magnetization values after stepwise demagnetization plot as a straight line that reaches nearly to the origin of an

orthogonal projection. Another third of the pilot specimens can be characterized as a type B magnetization, that is, they are multicomponent, and after stepwise demagnetization, one of these components shows
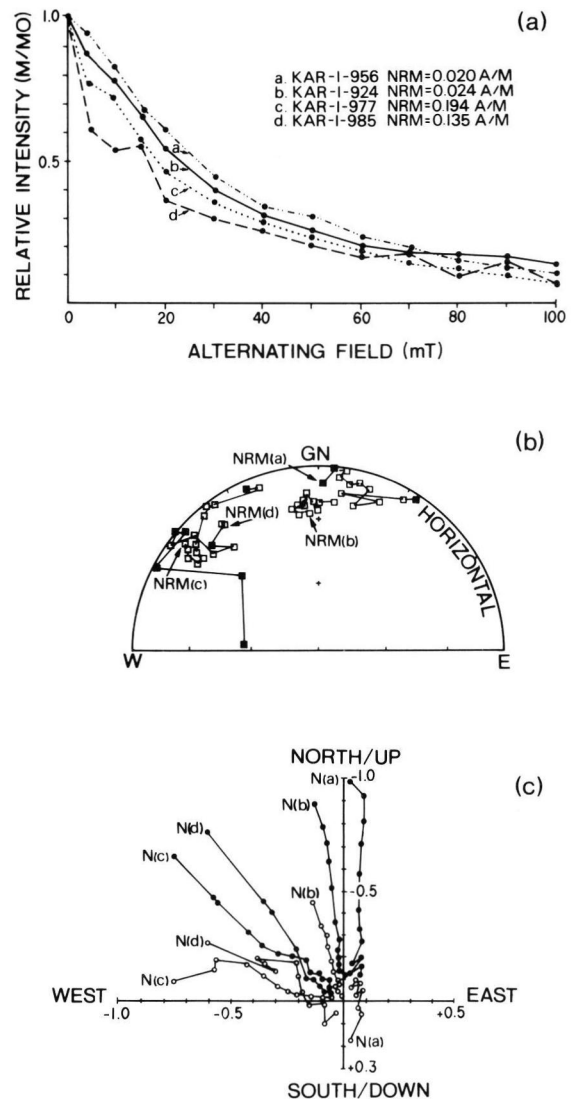

Fig. 5: Magnetization behavior of pilot specimens
from normally magnetized unconsolidated sediments
following stepwise alternating field (af) demagnetization.
Natural remanent magnetization is indicated by letters
NRM. Normalized magnetization (M/MO) versus af
demagnetization (a), and direction changes during a
demagnetization projected on a lower hemisphere equal area
stereographic projection (b) where open squares [□] and
solid squares [■] represent negative and positive inclination
respectively, and orthogonal vector projections (c),
with respect to present horizontal, where solid circles []
refer to N/S axis (horizontal plane) and open circles [00]
to Up/Down axis (vertical plane).

magnetization values which plot as a straight line that reaches nearly to the origin of an orthogonal projection. The remainder of the pilot specimens can be characterized as a type C magnetization, that is, they show incoherent magnetization values with stepwise demagnetization. The basalts beneath the Quaternary sediments show a single component (Type A) magnetization (Figure 6).

Type C magnetizations are recorded in sediments at 0—50 and 140—180 cm below the surface (Figure 7). These are zones containing abundant grit and pebble size tuff particles. The coarser fraction of these sedi-

(a)

Sample: KAR-I-O32
(vesicular basalt)
NRM = 1.68 A/M

(b)

(c)

Fig. 6: Magnetization behavior of a pilot specimen from the normally magnetized vesicular basalt found directly beneath the unconsolidated sediments. Symbols as in Figure 1.

ments is either too large for alignment in an ambient magnetic field and hence will show random magnetization directions, or was only partially aligned. In either case, the coarser fraction of the sediments may entirely or partially mask the dipole magnetization of the finer matrix fraction. In these sediments, stepwise demagnetization did not produce a clear direction with an end point near the origin of the orthogonal plot.

As can be seen from Figure 7, the inclination and declination profiles reveal a suite of normally magnetized sediments. The inclination profile shows a somewhat noisy record with values which in places are considerably steeper than would be expected for an equatorial sampling latitude. Inclination values at the equator should essentially be zero. Some of the large swings in declination and inclination are associated with low K^* values (Table 4), where K^* is a measure of the degree of internal consistency within a sample, and are thus suspect. K^* values greater than 10 are considered acceptable. The magnetization profile shows a rather consistent pattern of progressive waxing and waning of the sample intensity which in all likelihood is a true depiction of field behavior. This record would seem to indicate that the 2.4 meters of unconsolidated sediments at Karisoke were deposited over a period of several thousand years.
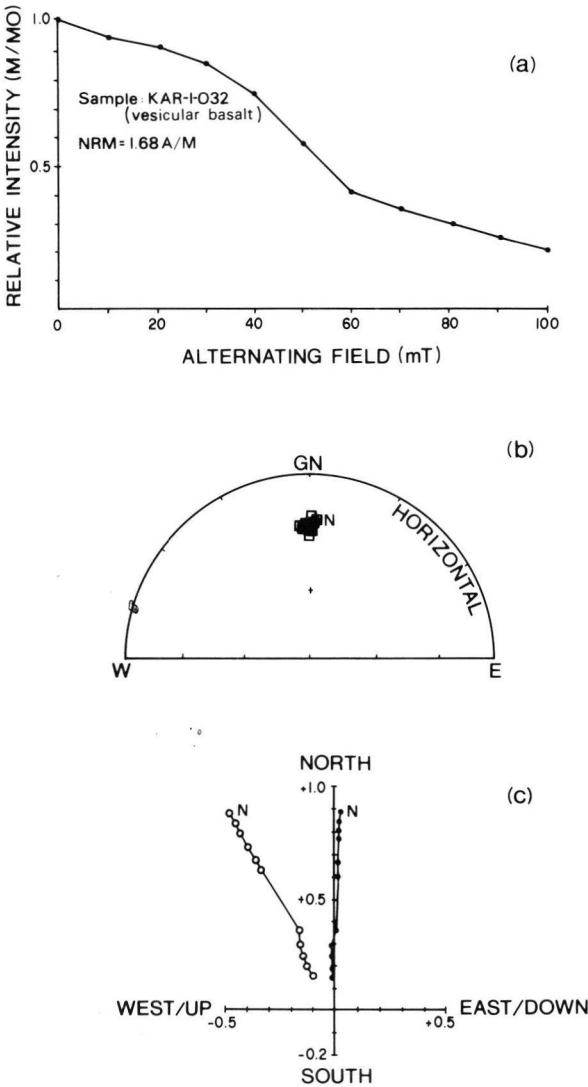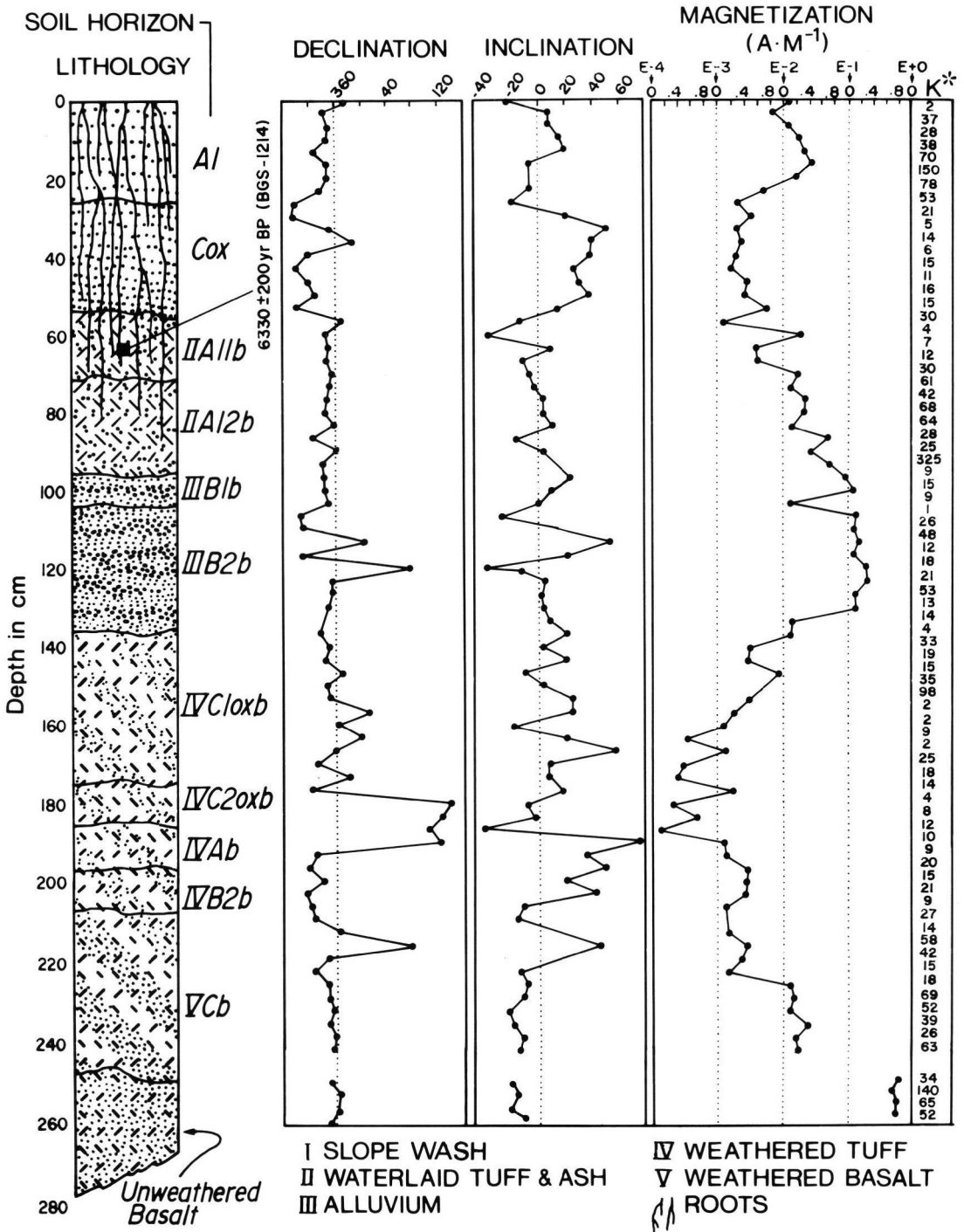
5 Conclusions

Two buried paleosols and one surface soil display different degrees of development compatible with genesis in: a) a drier stadial paleoclimate, b) wetter interstadial and early to middle postglacial paleoclimate, and c) drier later Holocene climate. The lithologic sequence of sediments supports the paleoclimatic interpretation in that alluvium (unit III) was emplaced between short — lived episodes of pyroclastic activity that emplaced tuffs (units IV and II). If the ^{14}C date of 6300 ± 200 yr BP is correct, it would appear the surface slope wash sediments buried the IIA11b horizon during the middle Holocene when the paleoclimate is known to have been wetter. However, in all likelihood the upper paleosol dates from the Kalambo Interstadial of the last glaciation.

The geochemistry of this sequence supports the notion of more intense weathering and translocation in the middle paleosol. In particular lower Na and Ca concentrations indicate more intense drainage and the data for Fe suggest displacement from the Ab complex into the B2b horizon in the middle paleosol. The data for U-Th indicate that radioactivity in the local bedrock is caused by both elements.

Fig. 7: Stratigraphic and paleomagnetic profiles for Site KAR 1, Virunga Mountains, Rwanda.
Magnetization values for all samples are at 10 militesla (mT) demagnetization.
Units of inclination and declination are in degrees; units of magnetization are in amperes per meter $A \cdot M^{-1}$.

Table 4: Mean Remanent Magnetization Directions

Site	Thickness	Lithology	Age	Polarity	N	M	D	I	K	α95	Pole Lat.	Pole Long.
Karisoke 1	250 cm	volcanic tuff & ash	Brunhes	N	73	.03	35	-0.5	11	7	81° N	303°
Karisoke 1	250 cm $^+$	vesicular	Brunhes	N	4	1.0	360	-23	298	5	80° N	206°

N   = number of specimens
M   = average intensity of magnetization (AM^{-1})
D   = average declination (degrees)
I   = average inclination (degrees)
K   = precision parameter (FISHER, 1953)
α95 = radius of the cone of 95 % confidence about the resultant vector

The Karisoke sediments are for the most part stably magnetized and record a normal dipole field. The zones of coarse sediment generally reveal incoherent magnetization directions which are nevertheless all normal. Mean remanent magnetization directions indicate a local field with an inclination of -0.5 degrees and a declination of 35 degrees indicating that a normal dipole field existed at the time of deposition of these sediments. The underlying vesicular basalt is likewise normally magnetized.

6 Acknowledgements

7 References

ANTRUM, P. & MAGNEE, L. (1983): Champ Volcanique des Birunga (map of bedrock in the Virunga Mountains). — Museum of Middle Africa, Tervuren, Belgium.

BIRKELAND, P. W. (1984): Soils and Geomorphology: N. Y., 372 p.; Oxford.

BOUYOUCOS, G. J. (1962): Hydrometer method improved for making particle size analyses of soils. — Agron. Jour. IV. 54, p. 464—465.

BOWER, C. A. & WILCOX, L. V. (1965): Soluble salts. — in BLACK, C. A., ed., Methods of Soil Analysis. — Madison, Wisc., Amer. Soc. Agron.: p. 933—951.

COE, M. J. (1967): The ecology of the Alpine zone of Mount Kenya. — The Hague, Junk, 136 p.

DAY, P. (1965): Particle fractionation and particle size analysis. — in BLACK, C. A. ed., Methods of Soil Analysis. — Madison, Wisc., Amer. Soc. Agron., p. 545—567.

FISHER, R. A. (1953): Dispersion on sphere. — Proc. of the Royal Soc., A 217, 295—305, London.

FOLK, R. L. (1968): Petrology of Sedimentary Rocks. — Austin, Texas, Hemphill Press, 170 p.

FOSSEY, D. (1982): Gorillas in the Mist. — 326 p., Houghton Mifflin Co., Boston Mass. Houghton Mifflin.

HANCOCK, R. G. V. (1978): Some aspects of the analyses of ancient artifacts by neutron activation analysis. — Jour. of Internatl. Inst. of Conservation — Candadian Group, 3 p.; Ottawa, Ont., 21—27.

— (1984): On the source of clay used for Cologne Roman pottery. — Archaeometry 26, p. 210—217; Oxford UK.

HARRIS, N. (1982): The Virunga Volcanoes. — unpublished notes on file at the Karisoke Research Centre, Virunga Mountains.

HEDBERG, O. (1964): Features of Afroalpine Plant Ecology. — Almquist and Wiksells, 144 p.; Uppsala.

MAHANEY, W. C. (1981): Paleoclimate reconstructed from paleosols: evidence from East Africa and the Rocky Mountains. — in MAHANEY, W. C. ed., Quaternary Paleoclimate. — Geobooks, p. 227—247; Norwich.

— (1988): Holocene glaciations and paleoclimate on Mount Kenya, East Africa: Quaternary Science Reviews, 7, 211—225.

MAHANEY, W. C. (1989b): Quaternary geology of Mount Kenya. — in MAHANEY, W. C., ed., Quaternary and environmental research on East African mountains. — 121—140; Balkema, Rotterdam.

— (1990): Glacially-crushed quartz grains in late Quaternary deposits in the Virunga Mountains, Rwanda — indicators of wind transport from the north. — Boreas, in press.

— (1990): Cadre stratigraphique géochronologique de la fin du Pleistocène et de l'Holocène dans le régions montagneuses de l'Est Africain. — L'Anthropologie, 2, 211—228; Paris.

— & BOYER, M. G. (1986): Microflora distributions in paleosols: a method for calculating the validity of radiocarbon-dated surfaces. — Soil Science, 142(2), p. 100—107.

MERCIER, A. (1984): Visité de la valleé à fond plateau entre le Bisoke et le Karisimbi. — Unpublished field notes.

OYAMA, M. & TAKEHARA, H. (1970): Revised Standard Soil Color Charts. — Japan Research Council for Agriculture, Forestry and Fisheries.

SOIL SURVEY STAFF (1951): Soil Survey Manual. — Washington, D. C., U. S. Department of Agriculture Handbook 18, U. S. Government Printing Office, 503 p.

— (1975): Soil Taxonomy: Washington, U. S. Government Printing Office, 754 p.

WHITTIG, L. D. (1965): X-ray diffraction techniques for mineral identification and mineralogical composition. — in BLACK, C. A., ed., Methods of Soil Analysis. — Amer. Soc. Agron., p. 671—696; Madison, Wisc.